Control Theory

Dennis Hens (r0852264)
Nick Hosewol (r0849415)

Assignment 1: Motor Identification

REPORT

Academic year 2023-2024

Contents

List of Figures

1 Selection of an appropriate model structure for the DC motors

Figure 1 shows a simple model for a DC-motor [1]. In this model v is the applied voltage, R and L are respectively the resistance and inductance of the motor, e is the back-EMF of the motor, T is the torque on the rotor, which has a moment of inertia equal to J. b is the constant of viscous friction. θ is the angular position of the rotor and $\dot{\theta} = \omega$ is the angular velocity, in terms of which the model is composed.

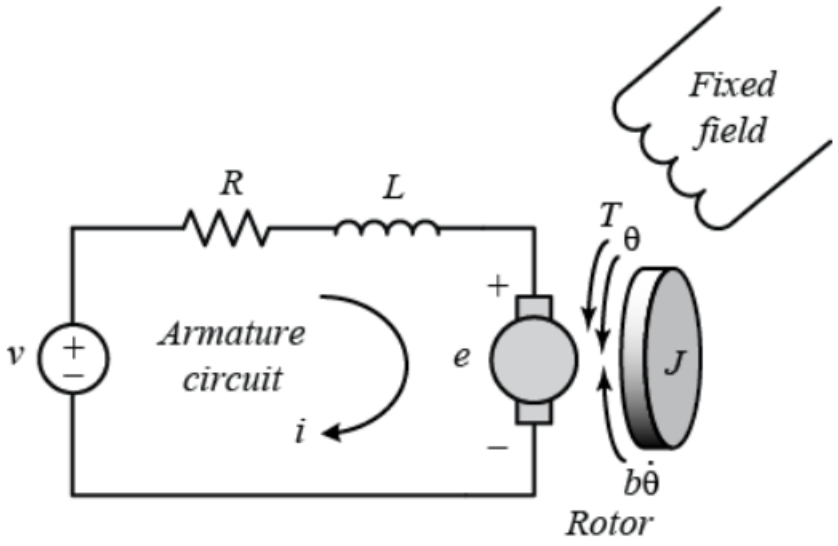

Figure 1: DC-motor model

Using the fact that $T = Ki$ and $e = K\dot{\theta}$ and applying Kirchoff's voltage law and Newton's second law, equation 1 is found.

$$\begin{cases} J\ddot{\theta} + b\dot{\theta} = Ki \\ L\frac{di}{dt} + Ri = v - K\dot{\theta} \end{cases} \tag{1}$$

Applying the Laplace transform yields equation 2.

$$\begin{cases} Js^2\Theta + bs\Theta = KI \\ (Ls + R)I = v - K\Theta \end{cases} \iff \begin{cases} \frac{\Omega(s)}{V(s)} = \frac{K}{(Js+b)(Ls+R)+K^2} \end{cases} \tag{2}$$

In this transfer function, $V(s)$ has the units of Vs, as this is the Laplace transform of $v(t)\,[V]$. Analogously, $\Omega(s)$, the Laplace transform of $\omega(t)\,[rad/s]$ has the units of $\frac{rad \cdot s}{s} = rad$, for the same reason. Physically, this transfer function related the voltage input $v(t)\,[V]$ on the DC-motor to its rotational velocity $\omega(t)\,[\frac{rad}{s}]$, which is taken to be the output.
As this transfer function is written in continuous time, the transfer function is discretised using a zero-order hold (ZOH) sampling process. Note that the earlier defined constants are replaced with random coefficients as the physical properties of the DC-motor are of no interest, only the transfer function is. The ZOH-equivalent is given by equation 3. Note that the sampling time is determined by the micro OS and equals $T_s = 10\,ms$.

$$H(z) = (1 - z^{-1})\mathcal{Z}(\mathcal{L}^{-1}(\frac{H(s)}{s})\delta_{T_S}(t)) \tag{3}$$

Using the Z-transform in figure 2, this leads to the form of equation 4 for the discretised transfer function.

Prototype 2nd order lowpass step response	$\frac{\omega_0^2}{s\left(s^2 + 2\zeta\omega_0 s + \omega_0^2\right)}$	$1 - \frac{1}{\sqrt{1-\zeta^2}} e^{-\zeta\omega_0 t} \sin\left(\omega_0\sqrt{1-\zeta^2}t + \phi\right)$ $\phi = \text{acos}(\zeta)$	$\frac{z}{z-1} - \frac{1}{\sqrt{1-\zeta^2}} \frac{z^2\sqrt{1-\zeta^2} + ze^{-\zeta\omega_0 T}\sin\left(\omega_0\sqrt{1-\zeta^2}T - \phi\right)}{z^2 - 2ze^{-\zeta\omega_0 T}\cos\left(\omega_0\sqrt{1-\zeta^2}T\right) + e^{-2\zeta\omega_0 T}}$ $\phi = \text{acos}(\zeta)$

Figure 2: table for the Z-transform

$$\frac{\Omega(z)}{V(z)} = \frac{az+b}{z^2+cz+d} \tag{4}$$

Now, as the micro OS also applies a delay between it's input and output, the transfer function needs to account for this phenomenon. This is achieved, by multiplying the transfer function with z^{-1}, as this introduces a delay element between the input and output of the system, yielding equation 5.

$$\frac{\Omega(z)}{V(z)} = \frac{az+b}{z^3+cz^2+dz} \tag{5}$$

This model has a numerator of order 1 and has a denominator of order three. Because the order of the denominator is two orders higher than that of the numerator, this model has two delays in total, one of which is to be attributed to the software system of the microOS.
This model, derived on physical grounds and discretised using a Zero-order hold scheme is the only one tested in this assignment. Some disregard the motor inductance as this is small with respect to the mechanical parameters, which would lead to a system with one order less in both numerator and denominator. This will be mentioned again later.

2 Excitation of the motors while holding the cart in the air

To determine the parameters of the model, a test voltage is applied to both motors of the cart. The pulse uses a square wave at $10\,V$, which lasts for one second, followed by a one-second duration at $0\,V$, and then a one-second application of $-10\,V$. This cycle repeats continuously. Due to the restriction of the input voltage at $12\,V$ and the aim to use a 'general' voltage level, the voltage input is selected to be $10\,V$ and $-10\,V$. The form of the input waves is chosen to excite a large range of relevant frequencies (which would not be achieved if a step function was chosen for example) and because it does not contain a DC-component, as this could induce low-frequency distortions. The waveform is repeated multiple the times, to average out the response of one of these pulses, to get a fitted model that is as accurate as possible. The input and the output of both motors are plotted in figure 3. In this figure, the output is zoomed in from $2.5s$ to $6.5s$ to provide a clearer view of the output angular velocity.

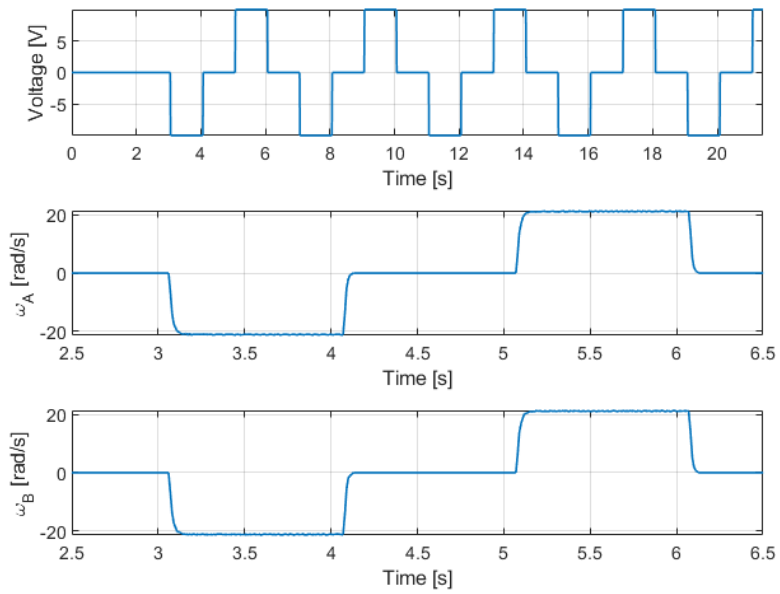

Figure 3: Input and output signal of motors A en B

3 Model parameter estimation

3.1 Estimation without filtering

To obtain the system parameters, which are the coefficients in equation 5, an ARX model structure is chosen. Equation 6 shows the relevant difference equation, based on equation 5. Note that the usual error term $e[k]$ is not included, as this term is not used further on.

$$\begin{aligned} & (z^3 + cz^2 + dz)\Omega = (az + b)V \\ \iff & (1 + cz^{-1} + dz^{-2})\Omega = (az^{-2} + bz^{-3})V \\ \iff & \omega[k] + c\omega[k-1] + d\omega[k-2] = av[k-2] + bv[k-3] \\ \iff & \omega[k] = -c\omega[k-1] - d\omega[k-2] + av[k-2] + bv[k-3] \end{aligned} \tag{6}$$

Such difference equations enable the notation of the ARX model parameter vector θ, the vector that contains all model parameters, and the regression vector $\phi(k)$, which contains all relevant input and output data. All these properties are summarised in table 1.

ARX Structure	**Model 1**
Difference equation	$\omega[k] + c\omega[k-1] + d\omega[k-2] = av[k-2] + bv[k-3]$
Regression vector	$\phi(k) = [-\omega[k-1], -\omega[k-2], v[k-2], v[k-3]]^T$
Parameter vector	$\theta = [c, d, a, b]^T$

Table 1: ARX model structure

The criterion on which the estimate for the parameters is based, is the *least squares criterion*. This criterion minimises the expression given by equation 7, where Z^N is the vector containing the measurement data, as shown in figure 3.

$$V_N(\theta, Z^N) = \Sigma_{k=1}^{N} \frac{1}{2}([y[k] - \phi^T[k] \cdot \theta)^2 \tag{7}$$

The solution to this least squares optimisation problem can be calculated using the pseudo inverse, or the *MATLAB* function $A\backslash b$, where A is the matrix containing all regression vectors, each row shifted by 1 value of k, until every measurement is used, as shown for a different example on slide 53 of C4 of [1]. b is the output vector, containing every measurement of ω.
This leads to an optimal value for the parameter vector θ. Equation 8 shows the transfer function for both motors, based on the data shown in figure 3.

$$\begin{aligned} & \theta_A = [-0.5393, 0.0373, 1.0812, -0.0323]^T \\ \iff & \frac{\Omega_A(z)}{V(z)} = \frac{1.081z - 0.0323}{z^3 - 0.5393z^2 + 0.0373z} \end{aligned} \tag{8}$$

$$\begin{aligned} & \theta_B = [-0.5886, 0.0578, 1.0602, -0.0724]^T \\ \iff & \frac{\Omega_B(z)}{V(z)} = \frac{1.06z - 0.07238}{z^3 - 0.5886z^2 + 0.05778z} \end{aligned}$$

Both of these transfer functions shown in equation 8 have a pole at $z = 0$, as expected: this is the manually added pole to compensate for the delay of the micro OS. Motor A has poles at $z = 0.4578$ and $z = 0.0815$, which correspond to frequencies at $f = 12.4344\,Hz$ and $f = 39.9032\,Hz$. The zero of motor A is located at $z = 0.0299$ which correspond to a frequency of $f = 55.8634\,Hz$. The other motor, motor B, has poles at $z = 0.4641$ and $z = 0.1245$, which correspond to frequencies at $f = 12.2160\,Hz$ and $f = 33.1598\,Hz$. The zero of motor B is located at $z = 0.0683$ which correspond to a frequency of $f = 42.6535\,Hz$. The (continuous) frequency, denoted p_c of these discrete poles, denoted p_d, was found using the formula in equation 9 [2].

$$\begin{aligned} p_c &= \frac{ln(p_d)}{Ts} \\ \iff p_d &= e^{p_c T_s} \end{aligned} \tag{9}$$

3.2 Impact of a Low pass filter

Figures 4a and 4b show the magnitude of the modelled transfer function on top of the transfer function derived from the measurement data. For higher frequencies, the measurement data seems mostly dominated by noise, which leads to the idea of filtering the measurement data, before using the data set to fit a transfer function. From the phase plots, figures 4c and 4d, it is also very clear that the real measurement data is completely dominated by noise at very high frequencies.

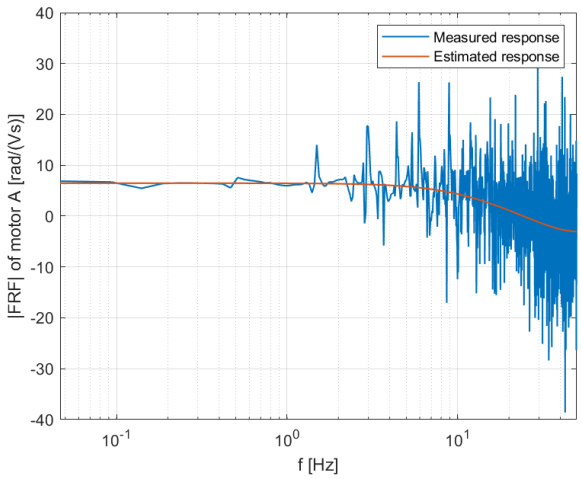

(a) Magnitude of the FRF of motor A

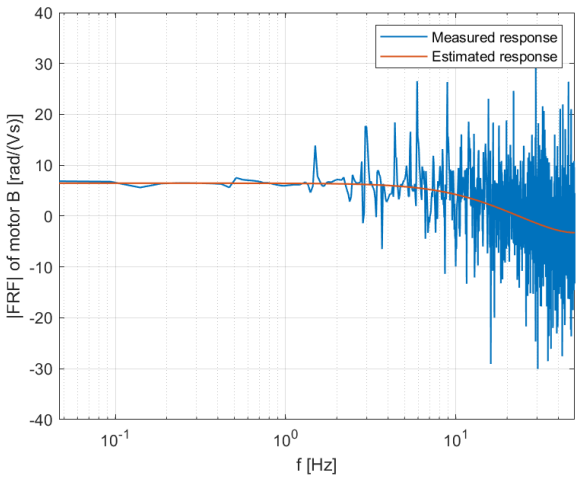

(b) Magnitude of the FRF of motor B

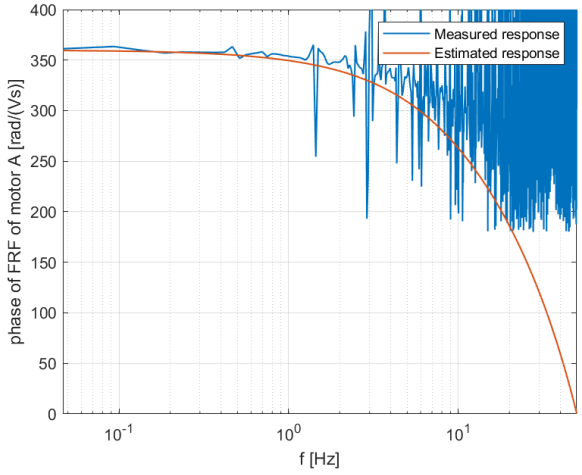

(c) Phase of the FRF of motor A

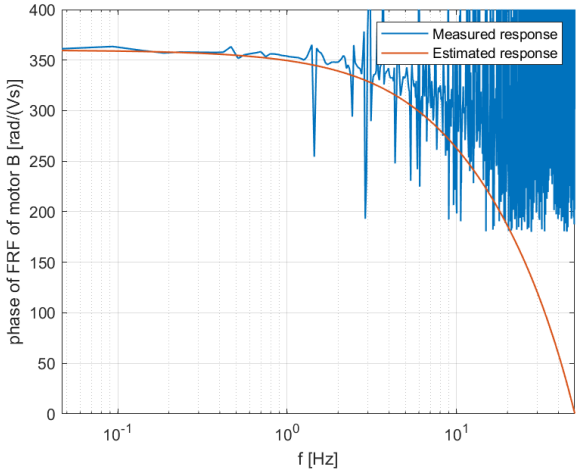

(d) Phase of the FRF of motor B

Figure 4: Empirical and estimated transfer functions for both motors

To effectively reduce the high-frequency noise, it is necessary to filter both the input and output signals. If only the output were filtered, the ratio of their frequency spectra, which is expected to represent the transfer function, which is supposed to represent the transfer function of the system, would be no longer the same. This, in turn, would be fitted to the model for the motor itself, resulting in an evidently incorrect outcome. Furthermore, as the prediction error is also a function of previous inputs (as is obvious from the difference equation 6), it is important to also filter the data on the inputs.
To design such a low-pass filter, the type of filter has to be chosen first. For this application, a Butterworth filter is chosen, due to its ease of implementation in *MATLAB*. Next, the order of the filter and the cut-off frequency have to be determined. The order of the filter has to be higher than the order of the system. To not overcomplicate the filter design and prevent an unnecessarily large overshoot an order of 6 is chosen. The cut-off frequency is chosen based on figure 4. Because the noisy part of the frequency response, still follows the general trend very well, the chosen cut-off frequency is chosen based on where the noise is very significant. This is chosen to be 20 Hz. It has to be noted that this cut-off frequency does lie before the fastest pole of both motors. However, since it is the slowest pole of the system that predominantly determines the transient behaviour and the cut-off frequency is chosen relatively far from the slowest pole, the negative effect of the

filter will be acceptable, thus rendering the chosen cut-off frequency as a great trade-off.

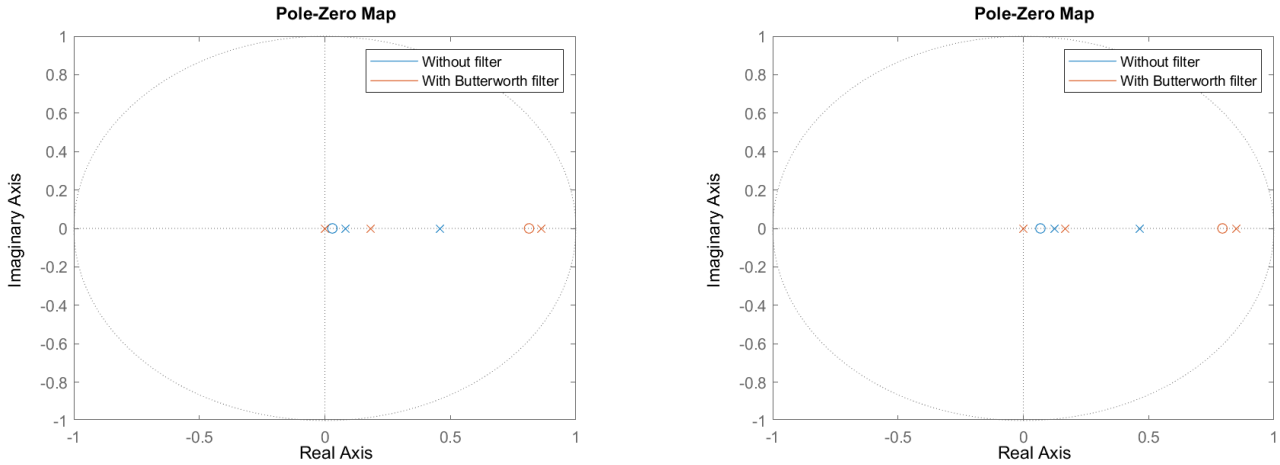

(a) Motor A

(b) Motor B

Figure 5: Pole-zero map of both motors with and without a filter

Figure 5 shows the pole zero map of both motors with and without the filter. The pole-zero map for motor A shows that both poles shifted to the right on the real axis, meaning that the poles shifted to lower frequencies. This slows the response of the system considerably. Furthermore, the zero of the system, is also shifted to a much lower frequency. The same observations are accurate for the filtered model of motor B. These observations are logical, as the high frequency information is attenuated, leading to lower frequency poles. Equation 10 shows the fitted models for the filtered data set.

$$\frac{\Omega_A(z)}{V(z)} = \frac{1.266z + 1.029}{z^3 - 1.044z^2 + 0.1567z}$$

$$\frac{\Omega_B(z)}{V(z)} = \frac{1.29z - 1.025}{z^3 - 1.015z^2 + 0.1416z} \tag{10}$$

Both of these transfer functions shown in equation 10 have a pole at $z = 0$, as expected: this is the manually added pole to compensate for the delay of the micro OS. Motor A has poles at $z = 0.8623$ and $z = 0.1817$, which correspond to frequencies at $f = 2.3585\ Hz$ and $f = 27.1399\ Hz$. The zero of motor A is located at $z = 0.8131$ which correspond to a frequency of $f = 3.2945\ Hz$. The other motor, motor B, has poles at $z = 0.8487$ and $z = 0.1668$, which correspond to frequencies at $f = 2.6111\ Hz$ and $f = 28.5035\ Hz$. The zero of motor B is located at $z = 0.7946$ which correspond to a frequency of $f = 3.6606\ Hz$.

3.3 Validation of the model

Sections 3.1 and 3.2 fitted 2 data sets, of which one was passed through a low-pass filter, for each motor to the proposed model. To validate their performance in reference to the real system, we estimate its step response using the proposed models, and compare these estimates to the measured step response. The step response is chosen to be a step of $10\,V$, as this is a common voltage in the operating range of the DC-motor.

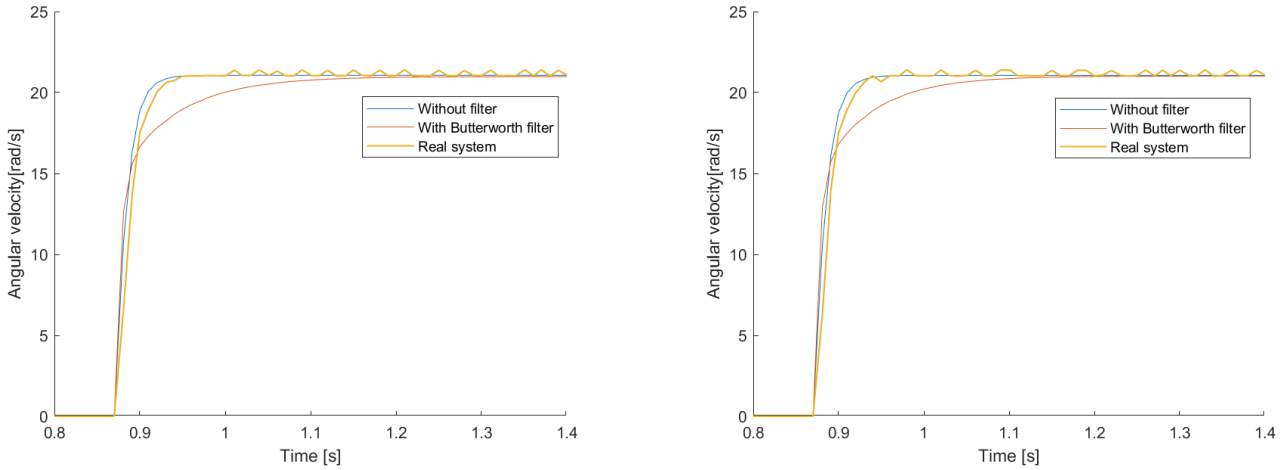

(a) Motor A

(b) Motor B

Figure 6: The measured and simulated response on a step input for both motors

Figure 6 shows the step responses of both the real system, the cart while held in the air, and of the proposed transfer functions. As shown in figure 6a, the original model, without the Butterworth filter, performs very well in the transient regime. This means the dominant pole of the first model correlates very well to the dominant pole of the real system. The filtered model performs less well, underestimating the speed of the system. This is logical, as the poles of the filtered system are considerably lower in frequency than the poles of the original model, leading to a slower response. For motor B, shown in figure 6b, all characteristics are very similar. Note that all models approach the correct steady state value.
Figure 7 show the difference between the real system response of both motors and the models which try to predict them. As discussed above, the filtered models clearly show a longer transient than the real system, while the unfiltered models don't. Both models underestimate the speed of the real system in the first few samples, but the error remains the largest in the unfiltered model.

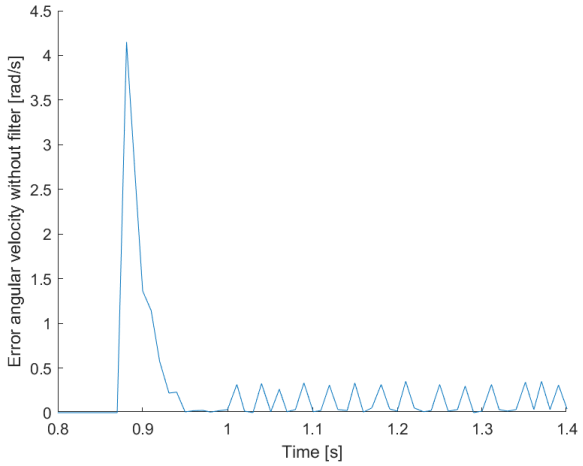

(a) Motor A without filter

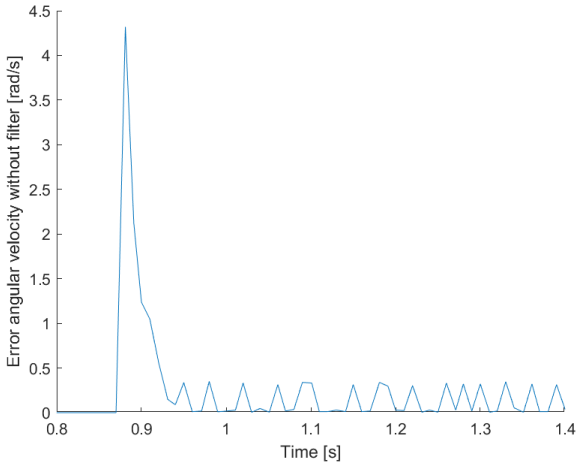

(b) Motor B without filter

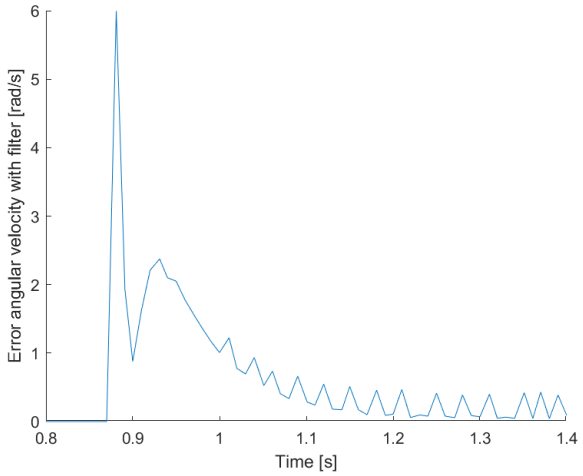

(c) Motor A with filter

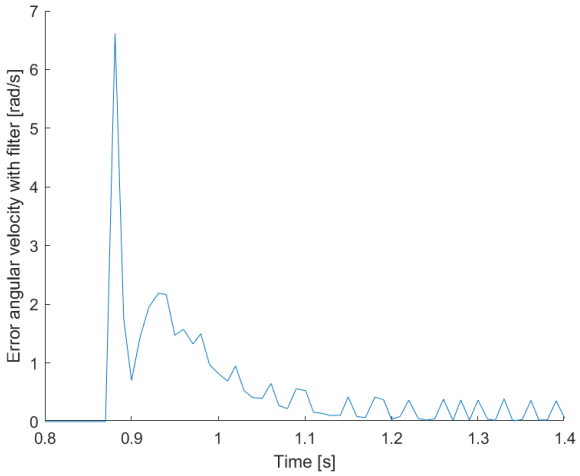

(d) Motor B with filter

Figure 7: Difference between the measured and simulated response in absolute value

In summary, the unfiltered model seems to perform better than the filtered model. This is possibly due to the chosen cut-off frequency of the Butterworth filter, which greatly alters the dominant pole of the system.

Another assumption which lies at the core of our modelling, is the fact that the system, the cart in the air, is a perfectly linear system (without this assumption, it is after all nonsensical to even talk about a transfer function or a linear difference equation). Equation 11 shows the main characteristics of a linear system. Let L be the operator which transforms an input voltage $v_i[k]$ into an angular rotation $\omega_i[k]$.

$$\begin{aligned} L(x_1[k] + x_2[k]) &= L(x_1[k]) + L(x_2[k]) = \omega_1[k] + \omega_2[k] \\ L(a \cdot v_i[k]) &= a \cdot L(v_i[k]) = a \cdot \omega_i[k] \end{aligned} \tag{11}$$

To test how linear the system behaves, the first property is checked for motor A (as the results would be very similar for motor B). Figure 8a plots the responses of the system to a step response of $3\,V$ and $7\,V$. These responses are added, and compared to the response of the system to a step of $10\,V$. If the system were linear, according to the first property in equation 11, the added response of the $3\,V$ and $7\,V$ signals should perfectly equal the response of the $10\,V$ signal. The error is also given in figure 8b.

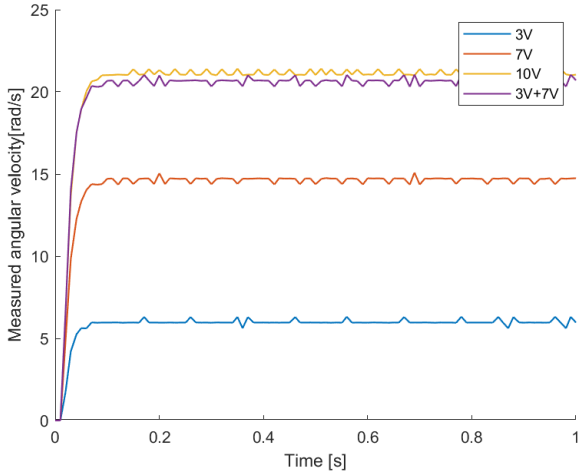

(a) Superposition

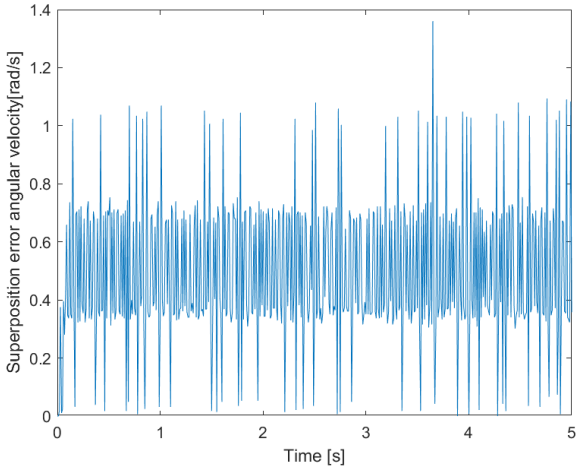

(b) Superposition error

Figure 8: Experimental analysis of the superposition principle

As seen from figure 8b, there is a clear non-zero average in the difference plot. This indicates that the system is definitely subjected to some non-linearity. However, the error is not too large for the operation range of the DC-motor, which implies that the linear models are definitely valid approximations. There are a few different sources for such non-linearities in a DC-motor, like mechanical friction in the bearings of the motor or the non-linear magnetisation curve of the iron core.
It is also noticeable that the total speed for a $10\,V$ is higher than the speed of the lower voltages combined. This implies that the sum of the non-linear friction effects is strictly higher than the non-linear friction effect of the summed voltage. Operating at higher voltages, therefore, would lead to relatively lower friction.

4 Ground validation of the cart system

This section validates the earlier models based on data gathered while the cart is actually in function.

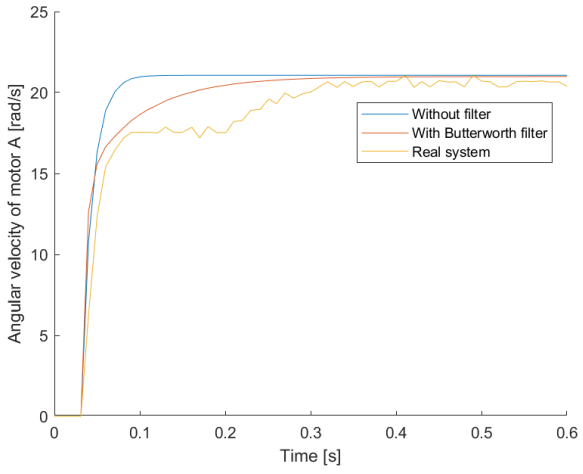

(a) Motor A

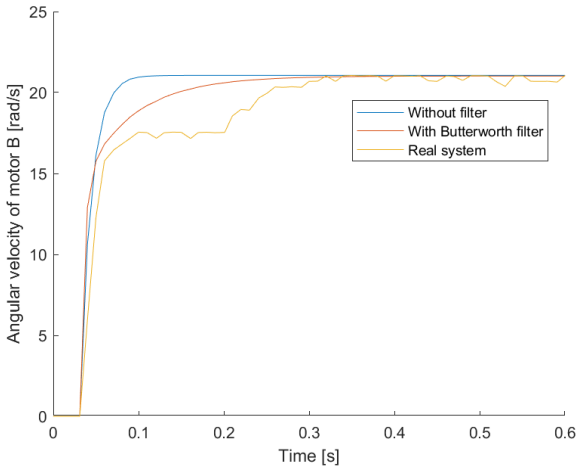

(b) Motor B

Figure 9: The measured and simulated response on a step input for both motors when the cart is placed on the ground

Figure 9 shows the predicted outputs for both models for the same $10\,V$ step input, as well as the measured output for the cart being on the ground, and thus driving forward. It is evident that the predicted outputs did not change with respect to the previous test, as nothing changed with the models. The measured output changed a lot in this case: Due to the whole cart being on the ground there are a lot of new forces on the motor + wheel system, such as a reaction force from the car body on the wheel (due to it having a mass), and

the friction forces on the ground. This leads to a plateau visible in the transient, needed to build up speed. (The first fast increase of rotational speed can be explained by the fact that the wheels might slip early on, until the frictional force builds up enough to move the full cart, but these effects are out of the scope of this analysis.) These combined effects lead to a general slower system.

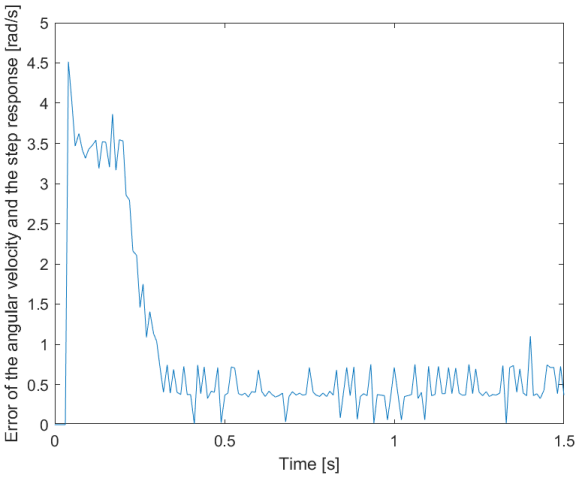

(a) Motor A without filter

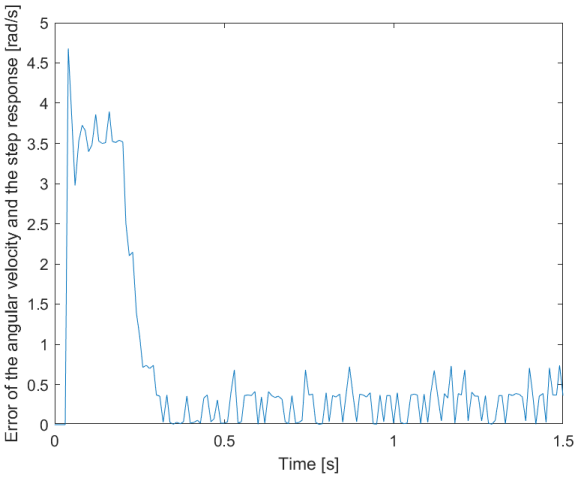

(b) Motor B without filter

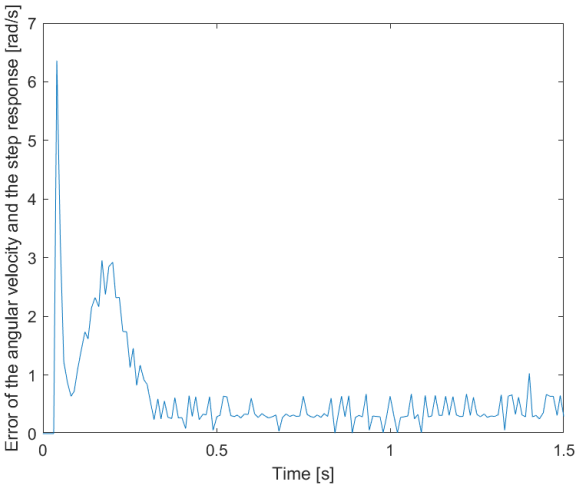

(c) Motor A with filter

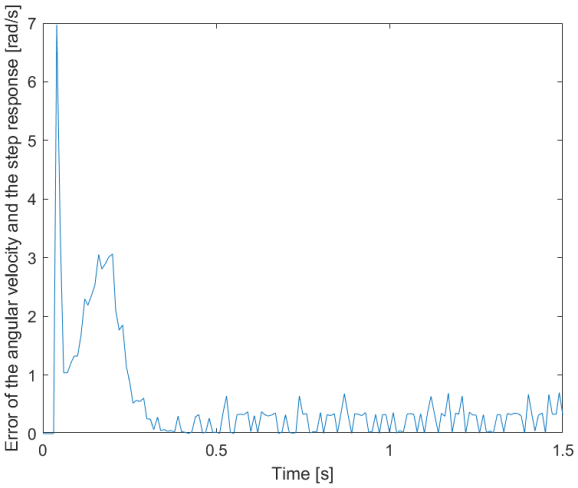

(d) Motor B with filter

Figure 10: Difference between the measured and simulated response in absolute value when the cart is placed on the ground

Figure 10 shows the difference between the filtered and unfiltered models and the real system response for motors A and B. As discussed earlier, the filtered model has a slower response than the unfiltered model, which, in the case of the cart driving on the ground matches the real systems measurements very closely, while the unfiltered model responds too fast.

The model structure presented in equation 5 is now re-identified to better fit the step response of the real, driving cart. The same excitation wave as in section 2 is chosen. The input waveform, as well as the output of both motors is shown in figure 11. In this figure, the output is zoomed in from $1s$ to $5s$ to provide a clearer view of the transition.

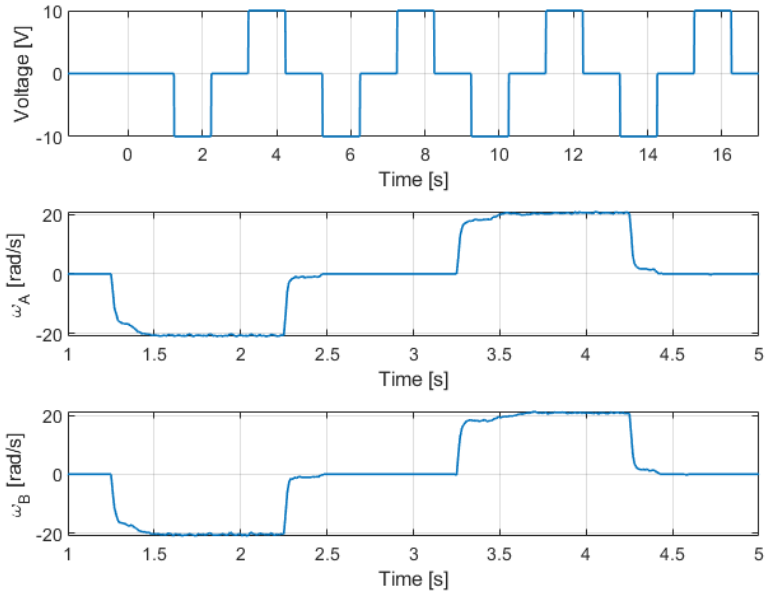

Figure 11: The input waveform with the output of both motors

The response of the system is very similar to the earlier responses in section 2. The plateau, which was mentioned earlier, is also clearly visible in the response to the wave pattern. This data can now be used to estimate the parameters in the model of equation 5. This data will not be passed through a low-pass filter, as, in the original modelling process, the filter did not have a positive effect on the step response. (The filter did have a positive effect for the ground measurements, but the original estimates were not based on the cart being on the ground, which explains the unfiltered models poor performance.) Furthermore, the approach of using unfiltered data is less complicated, as this does not require the tuning of a new Butterworth filter.
Using the exact same process as in section 3.1, new parameters are fitted to this data. Equation 12 shows these transfer functions, which will be used in the later assignments.

$$\begin{aligned} \frac{\Omega_A(z)}{V(z)} &= \frac{0.6466z - 0.07751}{z^3 - 0.9356z^2 + 0.2173z} \\ \frac{\Omega_B(z)}{V(z)} &= \frac{0.6886z - 0.1068}{z^3 - 0.9082z^2 + 0.1968z} \end{aligned} \tag{12}$$

The model for motor A have poles located at 0 Hz, 10.84 Hz and 13.45 Hz, using the same formula as in section 3.1. The zero is located at 33.76 Hz. For motor B, the poles are found at 0 Hz, 9.48 Hz and 16.38 Hz, while the zero is found at 29.66 Hz. The movement of the poles is shown in figure 12.

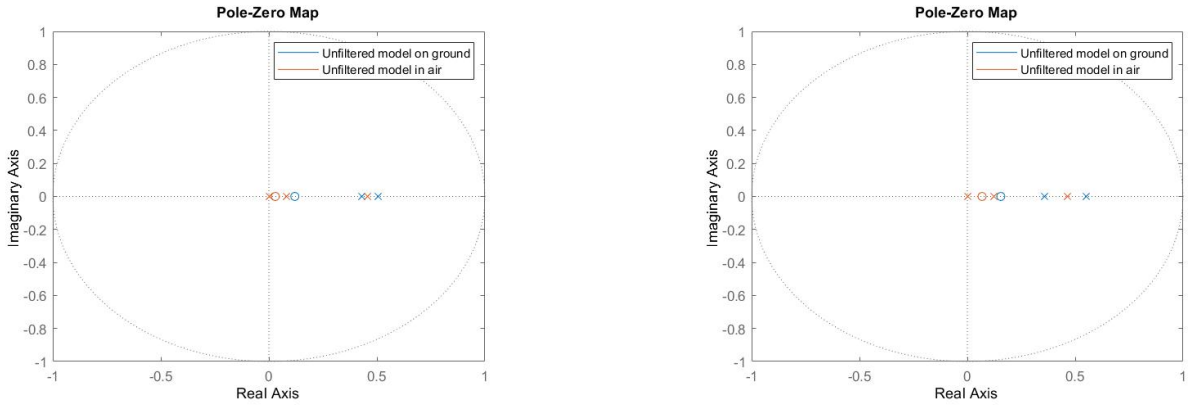

(a) Motor A

(b) Motor B

Figure 12: Pole-zero map of both motors with the cart placed on the ground

It is very noticeable that both poles for the two motors are now slower (and thus lower in frequency), due to the slower response of the cart on the ground. This is also very much in line with the qualitative expectation. The zeroes on the other hand, also move toward lower frequencies (as is to be expected), but not as much as the poles (definitely not as much as the faster poles from the previous models moved). This is a little unexpected, as the cart is put on the ground, the mechanical effects in the system increase greatly as discussed earlier, while the electrical inductance of the DC-motors contribute less (this is why the inductance is sometimes assumed to be zero, leading to a simpler model). This could lead to a pole zero-cancellation occurring in the model (therefore leading to said simpler model). This does, however, not happen in this fit, probably partially due to high frequency noise. The implementation of a low-pass filter would also decrease the frequency of the zero, probably leading to a cancellation.

References

[1] *DC Motor Speed: System Modeling*. URL: https://ctms.engin.umich.edu/CTMS/index.php?example=MotorSpeed&section=SystemModeling (visited on 11/06/2023).

[2] Pipeleers and Swevers. *Control Theory - handouts*. Aug. 2020.